The Canadian Mineralogist
Vol. 41, pp. 353-364 (2003)

A LAM–ICP–MS STUDY OF THE DISTRIBUTION OF GOLD IN ARSENOPYRITE FROM THE LODESTAR PROSPECT, NEWFOUNDLAND, CANADA

JOHN G. HINCHEY[¶], DEREK H.C. WILTON[§] AND MICHAEL N. TUBRETT

Department of Earth Sciences, Memorial University of Newfoundland, St. John's, Newfoundland A1B 3X5, Canada

ABSTRACT

The Lodestar prospect in eastern Newfoundland contains significant concentrations of Au within sulfide-mineralized, polylithic, magmatic-hydrothermal breccias. The highest grade was 58.5 g/t Au from a grab sample of massive arsenopyrite. Selective samples of other sulfide phases in the breccia, such as pyrite, however, failed to produce any comparatively anomalous Au values. We conclude that Au at the Lodestar prospect is directly related to the arsenopyrite. Sulfide-bearing samples were investigated using a variety of analytical techniques. Recent developments of *in situ* laser-ablation microprobe – inductively coupled plasma – mass spectrometry (LAM–ICP-MS) techniques have provided important insights into trace-element distributions in minerals. ICP–MS analyses were undertaken to determine whether Au is distributed homogeneously in sulfides, particularly arsenopyrite, or is contained as micronuggets. The LAM–ICP–MS results demonstrate that the Lodestar arsenopyrite contains Au concentrations that attain 201 g/t. Gold is "homogeneously" (*i.e.*, no nugget effect) contained within the structure of arsenopyrite. Other sulfide phases, such as pyrite and chalcopyrite, contain very low levels of Au. Gold contents in arsenopyrite from individual samples, and even within individual crystals, do vary, presumably related to arsenic concentrations. As gold was not observable by any of the other micro-analytical techniques, it must be chemically bound in the arsenopyrite structure, thereby classifying it as "invisible" gold.

Keywords: arsenopyrite, gold, solid solution, micronuggets, laser-ablation ICP–MS, Lodestar prospect, Newfoundland.

SOMMAIRE

L'indice de Lodestar, dans la partie orientale de Terre-Neuve, contient des concentrations importantes d'or dans des brèches magmatiques-hydrothermales polymictes minéralisées en sulfures. La teneur maximale, 58.5 g/t d'or, caractérise un échantillon quelconque d'arsénopyrite massive. Les échantillons d'autres minéraux du minerai sulfuré, la pyrite, par exemple, ne montrent pas de teneurs comparables. Nous en déduisons que l'or serait directement lié à l'arsénopyrite. Les échantillons contenant des sulfures ont été étudiés avec une batterie de techniques analytiques. Les développements récents d'analyse *in situ* par ablation au laser avec plasma à couplage inductif et spectrométrie de masse (LAM–ICP–MS) ont mené à de nouvelles observations à propos de la distribution des éléments traces dans les minéraux. Les analyses LAM–ICP–MS ont été faites pour déterminer si l'or est distribué de façon homogène dans les sulfures, en particulier l'arsénopyrite, ou s'il se présente sous forme de micropépites. Les résultats LAM–ICP–MS démontrent que l'indice Lodestar contient des concentrations d'or atteignant 201 g/t. L'or est réparti de façon homogène dans la structure de l'arsénopyrite, sans effet de micropépites. Les autres sulfures, la pyrite et la chalcopyrite, par exemple, contiennent des teneurs en or très faibles. Les teneurs en or de l'arsénopyrite dans des échantillons individuels varient, probablement en fonction des teneurs en arsenic. Parce que nous n'avons pas pu déceler l'or par les autres techniques micro-analytiques, cet élément doit être incorporé chimiquement dans la structure; on pourrait donc le qualifier d'or "invisible".

(Traduit par la Rédaction)

Mots-clés: arsénopyrite, or, solution solide, micropépites, ablation au laser avec analyse ICP–MS, indice de Lodestar, Terre-Neuve.

[¶] *Current address*: Department of Earth Sciences, University of Ottawa, 365 Nicholas Street, Ottawa, Ontario K1N 6N5, Canada.

[§] *E-mail address*: dwilton@esd.mun.ca

INTRODUCTION

The realization that gold in solid solution in sulfide minerals can reach economically exploitable concentrations has fueled attempts to understand the mechanisms by which gold is accommodated within specific sulfide minerals (*cf.* Cabri *et al.* 2000). Understanding of such processes is very important to economic geologists and mineral exploration companies, as it may provide a geochemically oriented approach for the targeting of economic gold deposits based on whether gold is freely distributed within the sulfides as a distinct phase, or is held within sulfide as so-called "invisible" or refractory gold. The understanding of the mineralogical characteristics of "invisible" gold is also important for successful processing of such ores.

The purpose of this experiment was to determine the nature and distribution of gold within the sulfide phases at the Lodestar prospect, Newfoundland. Initial techniques used in the study of the mineralization included ore microscopy, instrumental neutron-activation analysis (INAA), X-ray fluorescence (XRF), inductively coupled plasma – mass spectrometry (ICP–MS, solution mode), scanning electron microscopy (SEM), and electron-microprobe analysis (EMPA). We employed the ICP–MS instrument with a laser-ablation microprobe (LAM–ICP–MS) to analyze the arsenopyrite and coexisting sulfides for Au at the Lodestar prospect. Our goals were 1) to determine whether the gold is homogeneously distributed or contained in micronuggets, and 2) to gain insight into potential mechanisms that relate the Au and As as observed by INAA analysis. Tomkins & Mavrogenes (2001) have reported on the same approach to evaluate the importance of "invisible" gold in löllingite.

BACKGROUND INFORMATION

Results of the initial INAA assays indicate that there is a relationship between gold and arsenopyrite concentrations in the Lodestar suite. Although these data indicate that gold is relatively enriched in the arsenopyrite-rich samples, they did not give any precise information as to the nature or chemical distribution of the gold. The other techniques available were limited by detection limits or resolution abilities in their applicability to solve the problem, as there is no petrographically visible gold, and we could not locate the gold using SEM and EMPA results.

Other analytical techniques have been developed to detect "invisible" gold in arsenopyrite. These include Mössbauer spectrometry (Wu *et al.* 1990, Genkin *et al.* 1998), secondary-ion mass spectrometry (Cook & Chryssoulis 1990), X-ray photoelectron spectroscopy (XPS) (Fleet *et al.* 1993), and micro-X-ray absorption near-edge structure (XANES) (Cabri *et al.* 2000). These other techniques were unavailable to us for this study.

GEOLOGY OF THE LODESTAR PROSPECT

The island of Newfoundland represents the northeastern terminus of the Appalachian Orogenic Belt. The belt has been subdivided by Williams (1979) and Williams *et al.* (1988) into a number of tectonostratigraphic zones representing, from west to east, the Laurentian continental margin (Humber Zone), an internal mobile belt consisting of accreted oceanic, island arc and associated sedimentary terranes (the Dunnage Zone), and the Gondwanan continental margin (the Gander and Avalon zones).

Gold mineralization has been known from rocks of the Avalon Zone in the southern Appalachians for at least 200 years, as this area was the site of North America's first gold rush (Carpenter 1972). In these occurrences, gold is associated with hydrothermal systems in a variety of magmatic and structural settings related to epithermal, transitional, and porphyry systems (O'Brien *et al.* 1998). In the Avalon Zone of the Newfoundland Appalachians, however, auriferous mineralization has only been documented for the past two decades (*e.g.*, Taylor *et al.* 1979, O'Driscoll 1984), with numerous discoveries, and large, auriferous belts of hydrothermal alteration only recently delineated (*e.g.*, Dubé *et al.* 1998, Hayes & O'Driscoll 1990, Huard & O'Driscoll 1986, McKenzie 1986, O'Brien & O'Driscoll 1996, O'Brien *et al.* 1998, 1999).

In 1998, significant gold mineralization was discovered within polylithic breccia at the Lodestar Prospect. The best grades obtained by exploration companies from chip-channel sampling of the mineralized breccia consisted of 4.98 g/t Au and 14.8 g/t Ag over a 15.9 m width, with an assay of ~2.0% Zn. The highest-grade assays returned from the property (58.5 g/t Au with 260 g/t Ag) came from grab samples of massive arsenopyrite, as documented by the INAA method (Hinchey 2001).

This occurrence is associated with the Powder Horn Intrusive Suite (PHIS) in the Goobies area of the Avalon Peninsula (Fig. 1). The Powder Horn Intrusive Suite is a multiphase intrusive complex, with both pre- and post-brecciation phases. Pre-mineralization rocks consist of (1) sedimentary rocks of the late Neoproterozoic Musgravetown Group, which are transformed to hornfels close to the intrusion, (2) medium-grained gabbro and diorite, and (3) minor felsic material. The gabbro phase has been dated (U–Pb on zircon) at 603 ± 2 Ma. Post-mineralization phases include (1) fine-grained gabbro and diorite, (2) felsic phases, and (3) diabase dykes. A felsic dyke has been dated (U–Pb on zircon) at 605 ± 5 Ma.

The sulfide-mineralized breccia is exposed over approximately 20 m and contains gold in association with copper, arsenic and zinc sulfides. The sulfides form the matrix in parts of the breccia, whereas unmineralized parts of the breccia have a rock-flour or actinolite–chlo-

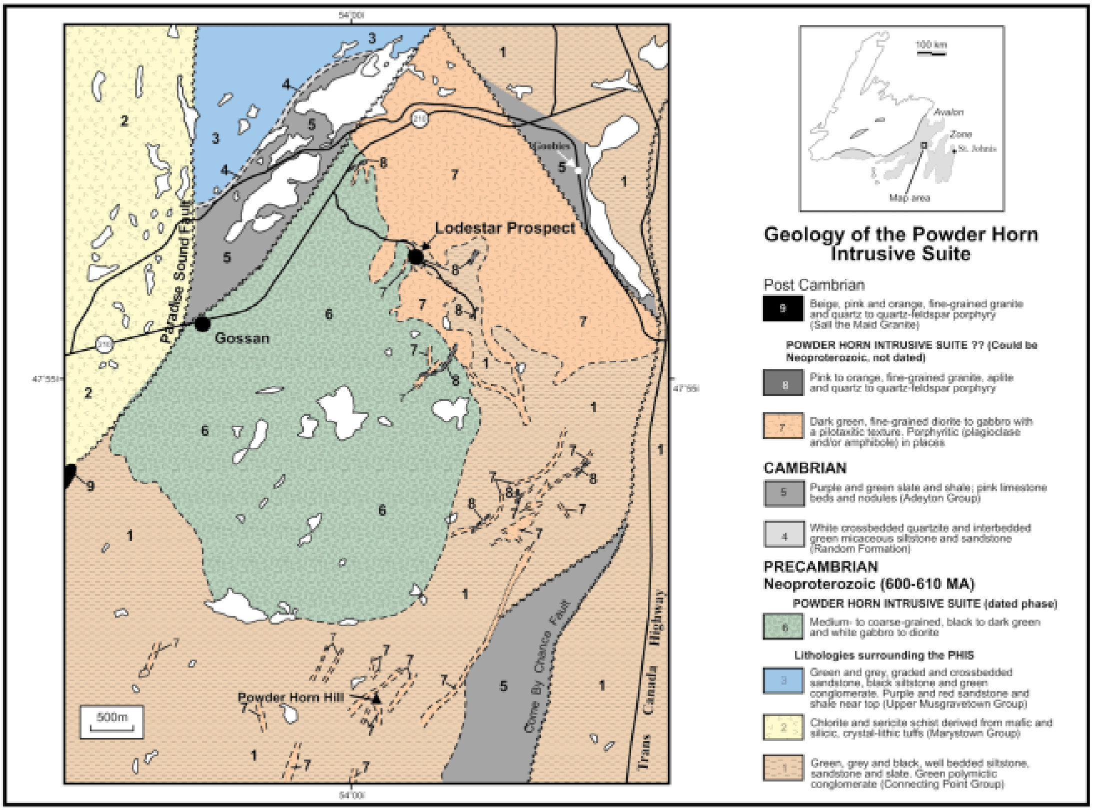

FIG. 1. Geology of the Powder Horn Intrusive Suite and surrounding area in eastern Newfoundland (Hinchey 2001).

rite matrix. The breccia contains rounded to angular clasts of sedimentary rocks, the early diorite and gabbro, quartz porphyry, quartz–feldspar porphyry, diabase and minor fine-grained granite. Clast size varies from <1 cm up to ~50 cm, but the clasts are typically <10 cm. The clasts of sedimentary rocks, gabbro and diorite were derived from the wallrocks of the breccia (Hinchey 2001).

The breccia is dominantly clast-supported, with varying amounts of matrix (~5 to 15%). The matrix consists of sulfides and oxides, chlorite – actinolite – tremolite, and rock flour, all of which vary in proportion throughout the breccia. Where mineralized, the matrix consists of arsenopyrite, pyrite, chalcopyrite, and magnetite, with minor amounts of bornite and sphalerite (Fig. 2). The matrix mineralization overprints, and is preferentially associated with, some of the breccia clasts, and is therefore assumed to be syn- to post-brecciation. The overprinting texture is predominantly associated with the quartz and quartz–feldspar porphyry clasts; sulfide mineralization, in the form of arsenopyrite and pyrite, is intergrown with the clasts, indicating chemical affinity between the sulfide mineralization and those clasts.

Within the breccia, the sulfide minerals are segregated into arsenopyrite-rich, pyrite-rich, and sphalerite-rich zones in which the sulfides occur as veinlets and semi-massive pods within the matrix (Fig. 3). This "segregation" of the various sulfide phases into veins and pods suggests a post-breccia mineralizing event.

Sulfur isotope and arsenopyrite geothermometers indicate that the temperature of mineralization was approximately 425°C; the sulfide minerals have a range of $\delta^{34}S$ values from +3.3 to +4.0‰ (Hinchey 2001).

Hinchey (2001) suggested that the Lodestar Prospect is a magmatic-hydrothermal breccia related to a porphyry system at depth. In particular, the breccia was derived from the explosive exsolution of fluid from a gold-bearing porphyry intrusive system at depth. Similar genetic models have been suggested for deposits such as Kidston (Baker & Andrew 1991, Baker & Tullemans 1990), Mount Leyshon (Paull *et al.* 1990), in Australia, and Golden Sunlight, in Montana (Porter & Ripley 1985).

The Concept of "Invisible" Gold

As reviewed by Cabri *et al.* (1989), the nature of gold within sulfide phases such as arsenopyrite and pyrite has been investigated in attempts to understand why certain gold ores are not directly amenable to a process of cyanidation. Gold is known to occur in a number of ways, such as: free particles as inclusions within sulfide minerals (nugget effect), chemical compounds (*e.g.*, Au–Ag tellurides), and solid solutions within sulfide phases. such as arsenopyrite and pyrite (so-called "invisible" or refractory gold) (Cabri *et al.* 1989, Cook & Chryssoulis 1990, Genkin *et al.* 1998). Cabri *et al.* (2000) found that "invisible" gold can occur in two different chemical forms within arsenopyrite, either as covalently chemically bound gold or in elemental form; the two modes of incorporation seem to be mutually exclusive.

In many cases, refractory auriferous sulfide-bearing ores can constitute the majority of the gold present in a deposit. Concentrations of "invisible" gold have been reported to attain 1.52 wt% (15,200 g/t) within arsenopyrite from the Villeranges deposit, France (Boirin 1987, Johan *et al.* 1989). Similar concentrations have been described within the Congress mine, British Columbia (Cook & Chryssoulis 1990), and up to 0.14 wt%

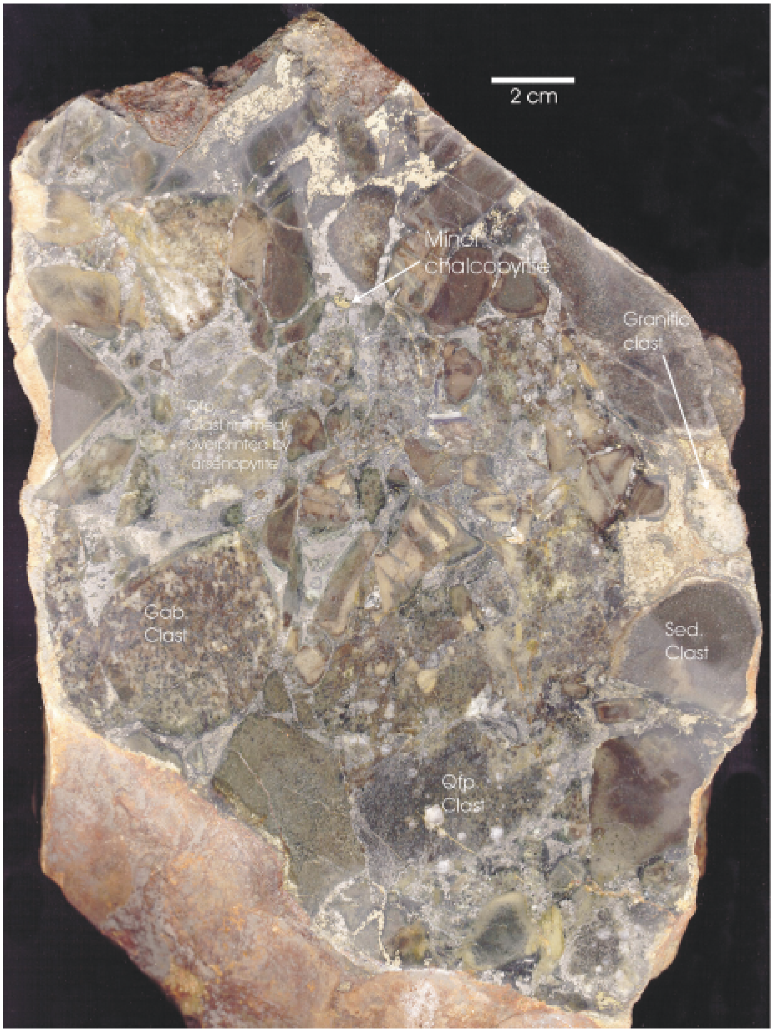

FIG. 2. Typical clast-supported breccia from the Lodestar prospect, with mineralization as matrix (Qfp: quartz–feldspar porphyry, Gab: gabbro, Sed: sedimentary).

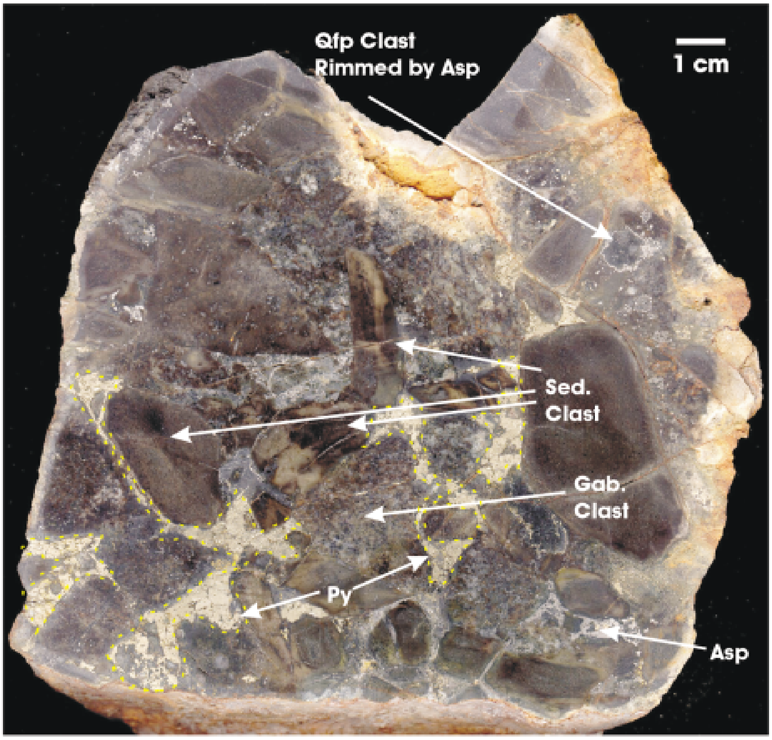

FIG. 3. Sulfides as veinlets and semimassive pods within the matrix at the Lodestar prospect. This "segregation" of the various sulfide phases within veins and pods suggest a post-breccia mineralizing event.

(1400 g/t) within natural pyrite (Fleet *et al.* 1993, Simon *et al.* 1999).

Controversy still exists regarding the mechanisms of incorporation responsible for the relationships between gold and arsenic within the structure of arsenopyrite and pyrite. Many mechanisms have been proposed for this substitution. Among these, 1) Au occupies the As sites in the arsenopyrite structure (Boyle 1979), 2) a substitution mechanism exists whereby 2As[Fe] substitute for (Au, Sb) + Fe (Johan *et al.* 1989), 3) a coupled substitution for arsenian pyrite that involves substitution of Au for Fe and As for S (Arehart *et al.* 1993), and 4) Au replaces As, but not Fe, in arsenopyrite and arsenoan pyrite (Genkin *et al.* 1988). Many other plausible mechanisms of substitution have been proposed. For the purposes of this summary, it is sufficient to say that substitution involves the replacement of As and Fe by Au.

INSTRUMENTATION AND DATA REDUCTION

Data for this study were obtained using an in-house-built 266 nm Nd:YAG laser system (Jackson *et al.* 1992) attached to a VG Fisons PlasmaQuad II+"S" quadrupole mass spectrometer at Memorial University of Newfoundland (MUN). The laser was focused 100–200 μm above the sample surface and fired at 10 Hz repetition rate using an energy of 0.3–0.5 mJ/pulse, depending on the concentration of the analytes in the samples. Data were acquired from both single-spot analyses (40 μm in diameter) and line rasters up to 0.8 mm in length. All measurements were performed in time-resolved analysis (TRA) – peak-jumping mode, with one point per mass peak. Dwell time was 8.3 ms, with a quadrupole settling time of 1 ms per mass. A typical acquisition consisted of a 40–60 s measurement of the gas background before the laser was switched on, followed by another 50–100 s of measurement with the laser on and material being ablated (Figs. 4, 5). Raw counts were processed off-line using the MUN-developed spreadsheet based program CONVERT to integrate signals from each sequential set of 10 sweeps. Data reduction and calculations of concentrations were then performed using the MUN-developed spreadsheet-based program LAMTRACE.

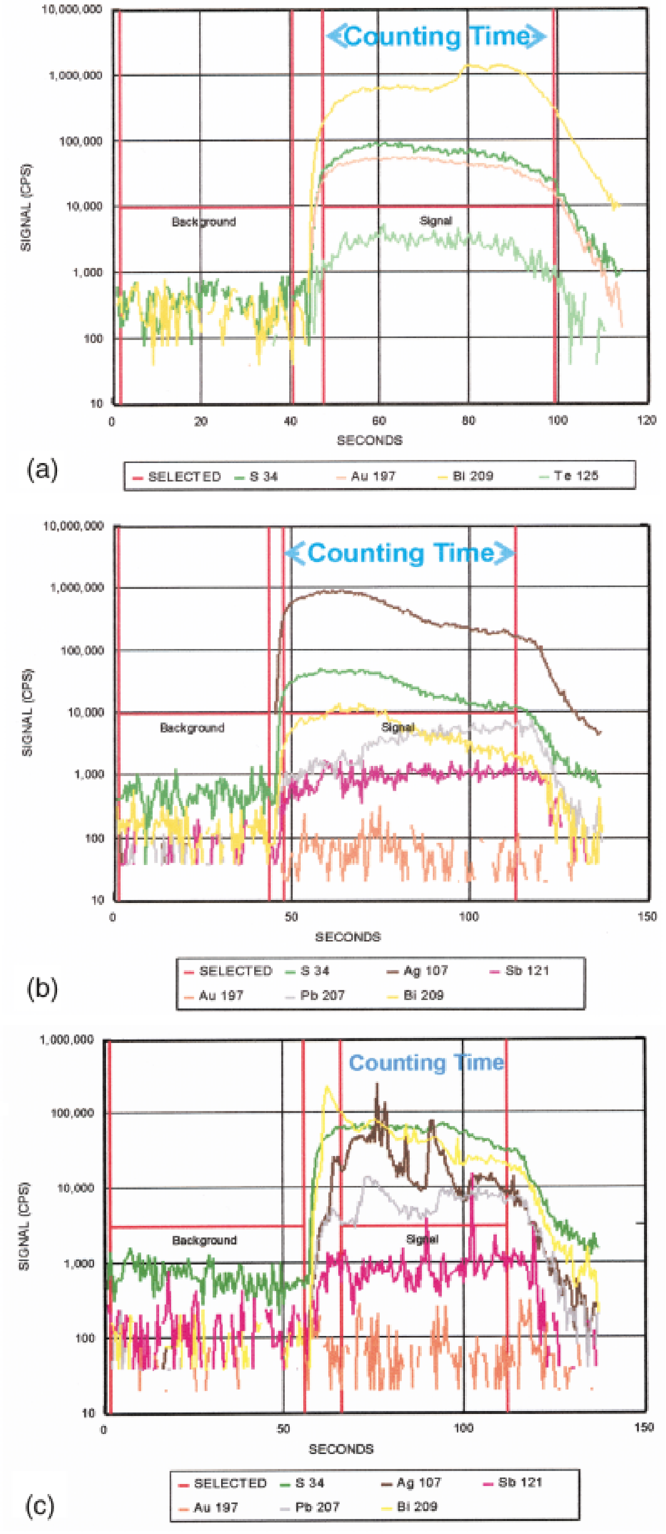

FIG. 4. Typical results recorded as counts per second (cps) *versus* time, obtained from single-spot ablation pits in the three sulfide phases at the Lodestar prospect: (a) arsenopyrite, (b) pyrite, and (c) chalcopyrite. Note the much higher Au counts acquired for the arsenopyrite, thereby suggesting a chemical association between As and Au.

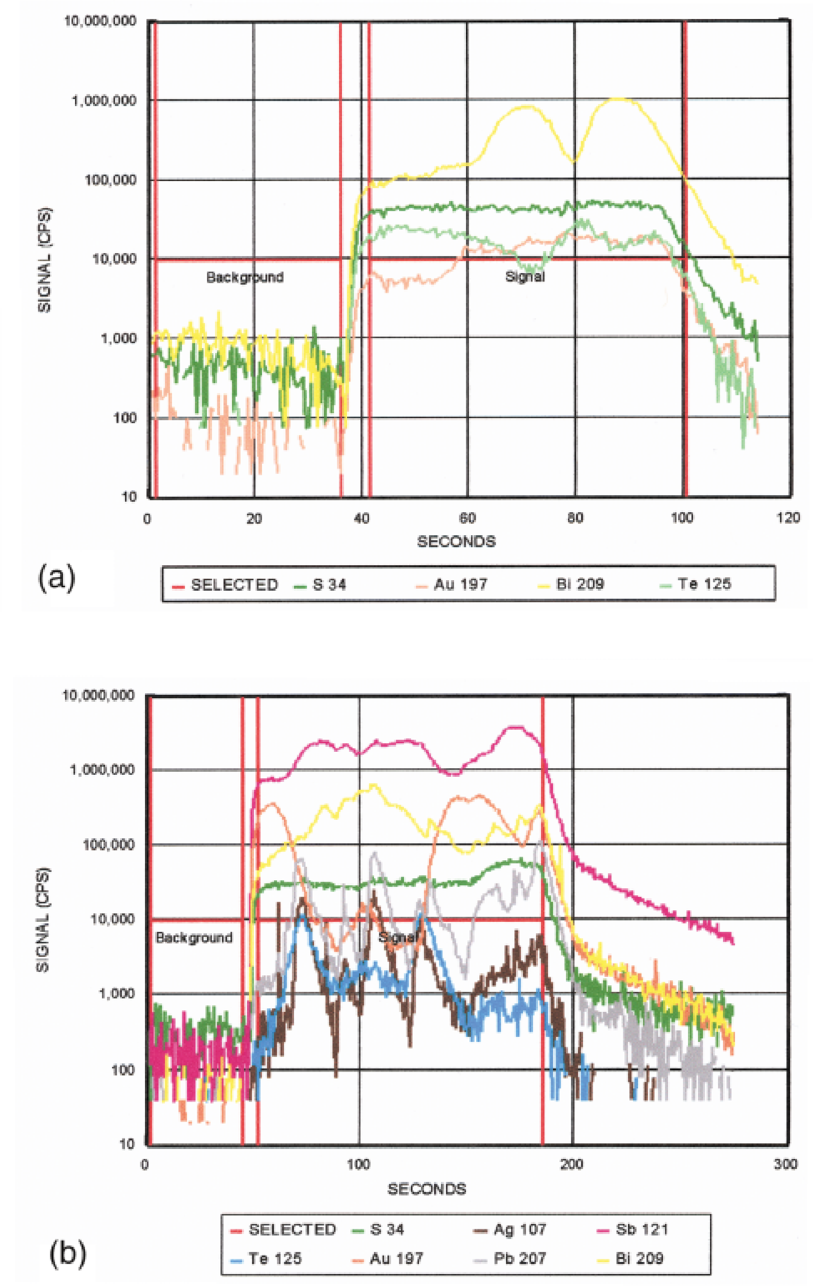

FIG. 5. Results obtained in counts per second (cps) *versus* time for two separate line-raster ablations within arsenopyrite. (a) This raster indicates a fairly flat signal, suggesting homogeneity. (b) This raster indicates that although the Au does not display a nugget effect, there is internal variation presumably related to crystal zoning and variations in proportions of As and Fe.

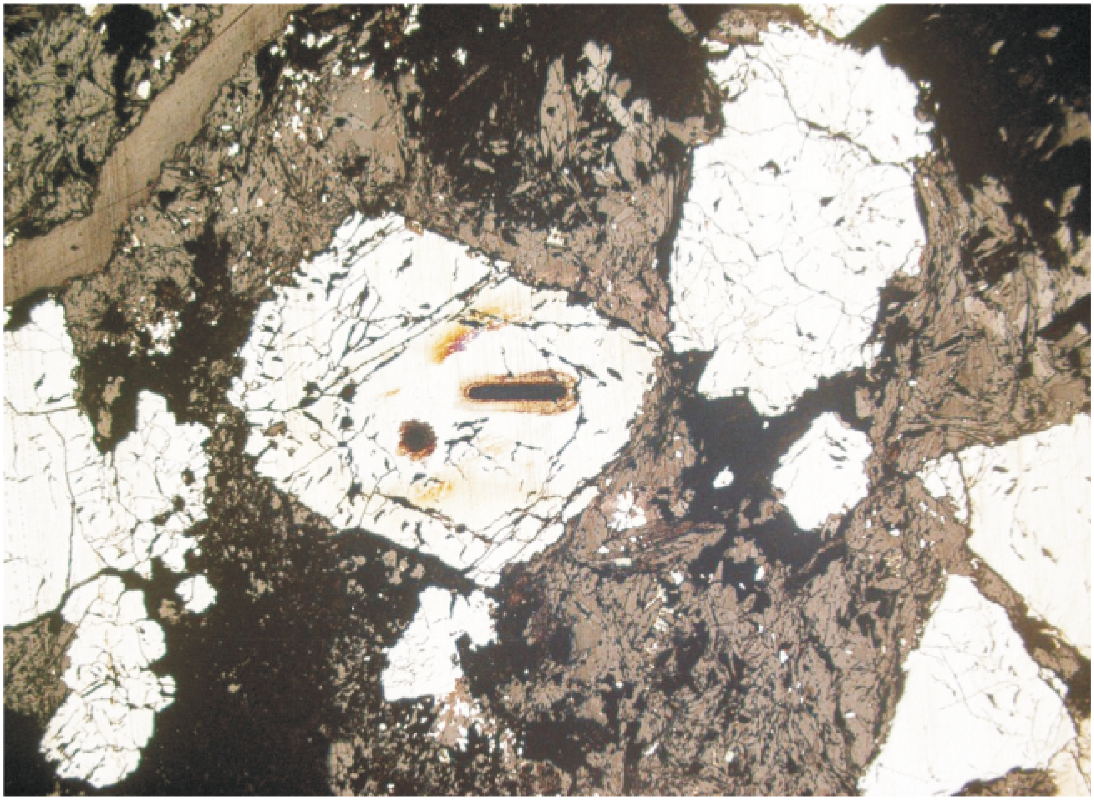

FIG. 6. Photomicrograph of single spot and line raster within a single crystal of arsenopyrite (JH99–MIN6; reflected light, 2.5×).

For quantitative analysis by LAM–ICP–MS, calibration is accomplished using an external calibration *via* a naturally occurring internal standard, usually a major element, that is present in both the calibration standard and the unknown mineral. This internal standardization corrects for the multiplicative effects of matrix, drift, and, most importantly in laser ablation, the quantity of sample ablated (*e.g.,* Longerich 2001). Use of an internal standard allows for calibration of one mineral matrix with another and for the use of varying energies of the laser to maximize signals from matrix to matrix. Sulfur was used as the internal standard in this study (Sylvester 2001), and its concentration was determined from electron-microprobe analyses (EMPA) of arsenopyrite, pyrite and chalcopyrite in the relevant sample. The equations for the calibration and sample concentration calculations, as used in this study, were discussed in detail by Longerich *et al.* (1996).

As an external standard for Au and S, we used a synthetic FeS standard containing 11.5 ppm of gold (Ballhaus & Sylvester 2000). No other elements (*e.g.,* Sb, Bi, Pb) could be quantified during the LAM–ICP–MS analyses owing to the lack of a suitable standard. The EMPA data were acquired on a Cameca SX–50 electron microprobe in the MUN laboratories. The automation software is SamX's "Xmas" for combined wavelength-dispersion (Cameca) and energy-dispersion (Oxford–Link) analyses.

For the purposes of the LAM–ICP–MS experiment, three representative thick polished sections of rock containing variable amounts of sulfides and variably-textured grains were chosen. The samples were labeled JH99–MIN6, JH99–MIN7 and JH99–MAT. All sulfide phases were analyzed to determine gold distribution throughout the mineralized showing. These sections, photographically documented, were also subjected to other analytical techniques, such as electron microprobe and scanning electron microscopy. Examples of the laser-ablation pits are shown in Figures 6 and 7.

RESULTS AND DISCUSSION

Results of electron-microprobe analyses (Table 1) indicate that As contents are variable in the arsenopyrite, ranging from 30.66 to 32.85%. The most significant differences are found from core to rim, and the largest variation was noted in arsenopyrite grains in sample MAT1, in which the As contents decrease 0.97% from core to rim. Zonation is also visible in back-scattered electron (BSE) images near the edge of one grain [JH99–MAT(1C2)]; the brighter areas contain over 1% more As than the darker zone (Table 1).

Data on counts per second (cps) *versus* time acquired from the LAM–ICP–MS indicate that the gold within the arsenopyrite occurs "homogeneously" within the structure, rather than being distributed as micronuggets. This observation is based upon the typically "flat", smooth cps data acquired from both single-spot and line-raster ablations (Figs. 4, 5), thereby indicating relatively small variations in the amount of gold distributed through the arsenopyrite at a single analytical point. In the LAM–ICP–MS analysis of the chalcopyrite grain illustrated in Figure 4c, however, Ag exhibits spikes in cps (at least partly coupled with an irregular distribution of Pb), which suggest that the laser intersected micro-inclusions while drilling through the sulfide.

Although Au appears to be homogeneous within the arsenopyrite (*i.e.*, not present as inclusions), there are wide variations in Au content within different grains of arsenopyrite (Table 2). Au concentrations vary from below detection limits in some grains up to 154, 152 and 162 ppm in samples JH99–MIN6, JH99–MAT and JH99–MIN7, respectively. Gold thus is zoned within individual crystals of arsenopyrite. Gold contents in pyrite and chalcopyrite intergrown with arsenopyrite (Table 2) are routinely low: ≤1.33 ppm in pyrite and ≤1.48 ppm in chalcopyrite.

Three short line-rasters from samples JH99–MAT and JH99–MIN7 are similar to the single-spot analyses in that Au is detected as a single, smooth cps line over the time-integrated ablation. Figure 5a from sample JH99–MIN7 is an example of one of these rasters. These rasters indicate that the Au cps are not spikey, and thus do not record the presence of Au as inclusions.

The longest (~0.8 mm) line-raster, as analyzed in sample JH99–MIN6 and illustrated in Figure 5b, however, displays significant spatial variation in Au contents, wherein the gold cps increase and decrease dramatically during the laser ablation of the arsenopyrite. To resolve the actual Au concentrations in some of these different spatial points, we integrated fewer time-slices to calculate contents from relevant peaks and troughs in Au cps. As listed in Table 2, these smaller intervals reveal Au contents ranging from 201 to 2.63 ppm along the raster.

In spite of these large spatial variations in Au contents, the data from the long raster-line are still interpreted to illustrate a dissolved gold content within the arsenopyrite (*i.e.*, no nugget effect). For instance, the smooth nature of the cps data argues against Au micronuggets, which would be observed as strong spikes in the signal. The raster-line variations, in fact, can be explained by analogy with the As variance as detected by EMP, in which these latter variations are considered to illustrate minor compositional zoning within the arsenopyrite structure, related to variable concentrations of As and Fe in the structure. Assuming that the Au is actually involved in a substitution relationship with As, this variability in As and Fe thereby determines how much gold can be incorporated within the structure of arsenopyrite.

Figure 5b also indicates that Au has antipathethic relationships with Bi and Sb, wherein Au troughs in the line-raster correspond to peaks in Sb and Bi. Gold thus is not present in micronuggets but in fact is chemically bound in the arsenopyrite, since micronuggets would cause random spikes in the relevant element, and would not produce concomitant decreases in other elements.

On the basis of the data acquired during this study, the most logical explanation as to how the gold is incorporated within the arsenopyrite structure at the Lodestar prospect is that Au substitutes for As and Fe in the mineral structure. However, more detailed work would be needed to quantify the role of each element (including Sb) in the substitution process.

CONCLUSIONS

The results obtained in this study serve to unambiguously illustrate a chemical affinity of the Au with arsenopyrite at the Lodestar prospect. It is dissolved in the arsenopyrite structure. Analyses obtained from both single-spot ablation pits and line-rastering indicate that gold preferentially occurs within the arsenopyrite structure compared to pyrite and chalcopyrite (Table 2, Fig. 5).

The results of this study indicate that the LAM–ICP–MS method can be an invaluable tool in the study of the nature and occurrence of precious-metal elements such as gold within ore-mineral phases. The instrument is capable of discerning the nature of such precious metals when they are held in an "invisible" state within the structure of the host minerals. In particular, the LAM–ICP–MS elucidated the nature of "invisible" Au within

TABLE 1. CONCENTRATIONS OF As, Fe AND S IN GRAINS OF ARSENOPYRITE FROM THE LODESTAR PROSPECT, NEWFOUNDLAND*

	As		Fe		S	
Sample	Core	Rim	Core	Rim	Core	Rim
MAT1		30.99		34.02		34.98
MAT1C3	32.01	31.04	33.92	33.84	34.07	35.09
MAT1C2 (dark)		30.66		33.90		35.41
MAT1C2 (light)		32.72		33.85		33.42
MIN7C3	32.85	32.68	32.63	32.67	34.52	34.63
MIN7C4	32.26	32.35	32.62	32.78	35.07	34.86
MIN7C7	32.32	32.84	33.35	32.48	34.32	34.68

* analyzed with an electron microprobe. Concentrations expressed in weight %.

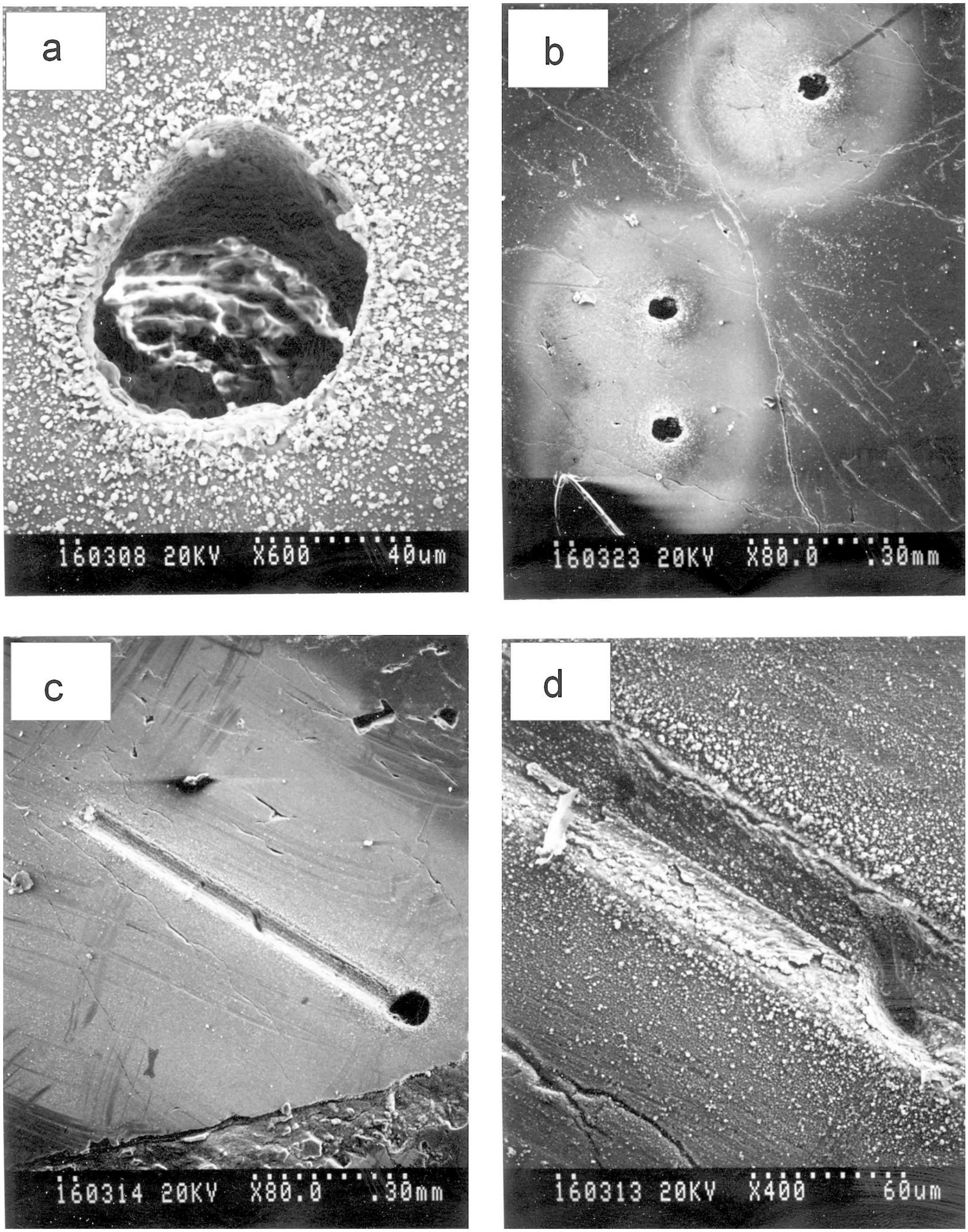

Fig. 7. Back-scattered electron (BSE) images from SEM, illustrating single-spot ablation pits (a, b) and line-raster pits (c, d) in arsenopyrite. Note the variable ablation within the line-raster, as illustrated in d (blowup of c).

TABLE 2. ABLATION RESULTS (LAM–ICP–MS) FOR Au IN ARSENOPYRITE, PYRITE AND CHALCOPYRITE, LODESTAR PROSPECT, NEWFOUNDLAND

	JH99-MIN6			JH99-MAT			JH99-MIN7
Spot	Asp	Py	Cpy	Asp	Py	Cpy	Asp
1	8.65			47.9			7.35
2	154			152			4.67
3	82.1			15.3			58.6
4	43.6			24.3			0.85
5	40.0			14.4*			7.90
6	31.9			1.31			12.2
7	72.9*			78.4			91.3
8	0.12			50.8			25.7
9	1.74			BDL			4.46*
10	126			BDL			31.1*
11		BDL			0.03		162
12		0.03			1.33		102
13		0.73				0.63	146
14			1.48				158
15			0.06				
Raster	JH99-MIN6						
P1	193						
T1	3.52						
P2	7.56						
T2	2.63						
P3	201						
T3	32.6						
P4	88.2						
RDL	0.012			0.005			0.004

* Raster: represents average values as calculated from the cps; BDL: below detection limit; RDL: run detection limit; P1: peak 1..... P4: peak 4, T1: trough 1.... T4: trough 4. The results are expressed in ppm.

arsenopyrite at the Lodestar prospect; an observation useful both from the exploration potential aspect and also for an understanding of the nature of the ore within the prospect. We suggest that the gold may be held *via* an elemental substitution of Au for As or Fe.

ACKNOWLEDGEMENTS

Funding for this project was provided by the Newfoundland Department of Mines and Energy; we thank Cyril O'Driscoll for discussions and continued support. Funding was also received from Wilton's NSERC Operating Grant. The extensive reviews by Louis J. Cabri, Robert F. Martin, Marc Norman and Paul Sylvester greatly aided us in improving the manuscript.

REFERENCES

AREHART, G.B., CHRYSSOULIS, S.L. & KESLER, S.E. (1993): Gold and arsenic in iron sulfides from sediment-hosted disseminated gold deposits: implications for depositional processes. *Econ. Geol.* **88**, 171-185.

BAKER, E.M. & ANDREW, A.S. (1991): Geologic, fluid inclusion, and stable isotope studies of the gold-bearing breccia pipe at Kidston, Queensland, Australia. *Econ. Geol.* **86**, 810-830.

________ & TULLEMANS, F.J. (1990): Kidston gold deposit. *In* Geology of the Mineral Deposits of Australia and Papua New Guinea 2 (F.E. Hughes, ed.). *Austral. Inst. Mining Metall., Monogr.* **14**, 1461-1465.

BALLHAUS, C. & SYLVESTER, P. (2000): Noble metal enrichment processes in the Merensky Reef, Bushveld Complex. *J. Petrol.* **41**, 545-561.

BOIRIN, M.C. (1987): Minéralisations à Au, As, Sb, altérations hydrothermales et fluides associés dans le bassin de Villeranges (Combrailles, Massif Central Français). *Université Nancy, Géologie, Geochimie et Uranium, Mém.* **15**.

BOYLE, R.W. (1979): The geochemistry of gold and its deposits. *Geol. Surv. Can., Bull.* **280**.

CABRI, L.J., CHRYSSOULIS, S.L., DE VILLIERS, J.P.R., LAFLAMME, J.H.G. & BUSECK, P.R. (1989): The nature of "invisible" gold in arsenopyrite. *Can. Mineral.* **27**, 353-362.

________, NEWVILLE, M., GORDON, R.A., CROZIER, E.D., SUTTON, S.R., MCMAHON, G. & JIANG, DE-TONG (2000): Chemical speciation of gold in arsenopyrite. *Can. Mineral.* **38**, 1265-1281.

CARPENTER, P.A. III (1972): Gold resources of North Carolina. *North Carolina Dep. of Nat. and Econ. Resources, Inform. Circ.* **21**.

COOK, N.J. & CHRYSSOULIS, S.L. (1990): Concentrations of "invisible" gold in the common sulfides. *Can. Mineral.* **28**, 1-16.

DUBÉ, B., DUNNING, G. & LAUZIÈRE, K. (1998): Geology of the Hope Brook mine, Newfoundland, Canada: a preserved late Proterozoic high-sulphidation epithermal gold deposit and its implications for exploration. *Econ. Geol.* **93**, 405-436.

FLEET, M.E., CHRYSSOULIS, S.L., MACLEAN, P.J., DAVIDSON, R. & WEISENER, C.G. (1993): Arsenian pyrite from gold deposits: Au and As distribution investigated by SIMS and EMP, and color staining and surface oxidation by XPS and LIMS. *Can. Mineral.* **31**, 1-17.

GENKIN, A.D., BORTNIKOV, N.S., CABRI, L.J., WAGNER, F.E., STANLEY, C.J., SAFONOV, Y.G., MCMAHON, G., FRIEDL, J., KERZIN, A.L. & GAMYANIN, G.N. (1998): A multidisciplinary study of invisible gold in arsenopyrite from four mesothermal gold deposits in Siberia, Russian Federation. *Econ. Geol.* **93**, 463-487.

HAYES, J.P. & O'DRISCOLL, C.F. (1990): Regional geological setting and alteration within the eastern Avalon high-alumina belt, Avalon Peninsula, Newfoundland. *Nfld. Dep. of Mines and Energy, Rep.* **90–1**, 145-155.

HINCHEY, J.G. (2001): *An Integrated Geochemical, Petrologic, Geochronological, and Metallogenic Study of the Powder Horn Intrusive Suite and the Associated Lodestar Prospect – a Magmatic-Hydrothermal Auriferous Breccia Zone that Links Epithermal and Porphyry Systems, Northern Burin Peninsula, Newfoundland.* M.Sc. thesis, Memorial University of Newfoundland, St. John's, Newfoundland.

HUARD, A. & O'DRISCOLL, C.F. (1986): Epithermal gold mineralization in Late Precambrian volcanic rocks on the Burin Peninsula. *Nfld. Dep. of Mines and Energy Rep.* **86–1**, 65-78.

JACKSON, S.E., LONGERICH, H.P., DUNNING, G.R. & FRYER, B.J. (1992): The application of laser-ablation microprobe – inductively coupled plasma – mass spectrometry (LAM–ICP–MS) to *in situ* trace-element determinations in minerals. *Can. Mineral.* **30**, 1049-1064.

JOHAN, Z., MARCOUX, E. & BONNEMAISON, M. (1989): Arsenopyrite aurifère: mode de substitution de Au dans la structure de FeAsS. *C.R. Acad. Sci. Paris* **308**, 185-191.

LONGERICH, H.P. (2001): Chemometrics. *In* Laser-Ablation–ICPMS in the Earth Sciences: Principles and Applications (P. Sylvester, ed.). *Mineral. Assoc. Can., Short Course Ser.* **29**, 21-28.

________, JACKSON, S.E. & GÜNTHER, D. (1996): Laser ablation inductively coupled plasma mass spectrometric transient signal data acquisition and analyte concentration calculation. *J. Anal. Atomic Spectrom.* **11**, 899-904.

MCKENZIE, C.M. (1986): Geology and mineralization of the Chetwynd deposit, southwestern Newfoundland, Canada. *In* Proc. Gold '86, Int. Symp. on the Geology of Gold (A.J. Macdonald, ed.). 137-148.

O'BRIEN, S.J., DUBÉ, B., O'DRISCOLL, C.F. & MILLS, J. (1998): Geological setting of gold mineralization and related hydrothermal alteration in late Neoproterozoic (post-640 Ma) Avalonian rocks of Newfoundland, with a review of coeval gold deposits elsewhere in the Appalachian Avalonian belt. *Nfld. Dep. Mines and Energy, Rep.* **98–1**, 93-124.

________, ________, ________ & ________ (1999): High sulphidation, epithermal-style hydrothermal systems in late Neoproterozoic Avalonian rocks on the Burin Peninsula, Newfoundland: implications for gold exploration. *Nfld. Dep. Mines and Energy, Rep.* **99–1**, 275-296.

________ & O'DRISCOLL, C.F. (1996): Preliminary investigation of Neoproterozoic (Avalonian) rocks, northeastern Holyrood (NTS 1N/6) map area: notes on geology, mineralization and mineral exploration potential. *Nfld. Dep. Mines and Energy, Rep.* **96–1**, 311-327.

O'DRISCOLL, C.F. (1984): The Hickey's Pond Belt; auriferous specularite – alunite – pyrophyllite – sericite mineralization near Placentia Bay, Newfoundland. *Nfld. Dep. Mines and Energy, Open File Rep.* **1M/16 (221)**.

PAULL, P.L., HODKINSON, I.P., MORRISON, G.W. & TEALE, G.S. (1990): Mount Leyshon gold deposits. *In* Geology of the Mineral Deposits of Australia and Papua New Guinea 2. *Austral. Inst. Mining Metall., Monogr.* **14**, 1471-1481.

PORTER, E.W. & RIPLEY, E. (1985): Petrologic and stable isotope study of the gold-bearing breccia pipe at the Golden Sunlight deposit, Montana. *Econ. Geol.* **80**, 1689-1706.

SIMON, G., KESLER, S.E. & CHRYSSOULIS, S. (1999): Geochemistry and textures of gold-bearing arsenian pyrite, Twin Creeks, Nevada: implications for deposition of gold in Carlin-type deposits. *Econ. Geol.* **94**, 405-421.

SYLVESTER, P.J. (2001): A practical guide to platinum-group element analysis of sulphides by Laser-Ablation–ICPMS. *In* Laser-Ablation–ICPMS in the Earth Sciences: Principles and Applications (P. Sylvester, ed.). *Mineral. Assoc. Can., Short Course Ser.* **29**, 203-211.

TAYLOR, S.W., O'BRIEN, S.J. & SWINDEN, H.S. (1979): Geology and mineral potential of the Avalon Zone and granitoid rocks of eastern Newfoundland. *Nfld. Dep. Mines and Energy, Rep.* **79–3**.

TOMKINS, A.G. & MAVROGENES, J.A. (2001): Redistribution of gold within arsenopyrite and löllingite during pro- and retrograde metamorphism: application to timing of mineralization. *Econ. Geol.* **96**, 525-534.

WILLIAMS, H. (1979): Appalachian Orogen in Canada. *Can. J. Earth Sci.* **16**, 792-807.

________, COLMAN-SADD, S.P. & SWINDEN, H.S. (1988): Tectonic-stratigraphic subdivisions of central Newfoundland. *Geol. Surv. Can., Pap.* **88–1B**, 91-98.

WU, X., DELBOVE, F. & TOURAY, J.C. (1990): Conditions on formation of gold-bearing arsenopyrite: a comparison of synthetic crystals with samples from Le Châtelet gold deposit, Creuse, France. *Mineral. Deposita* **25**, S8-S12.

Received February 25, 2002, revised manuscript accepted April 2, 2003.